

Superhumps Behavior during Normal Outbursts in ER UMa: Spectroscopy and Photometry

Yinghe Zhao, Zongyun Li, Xiaoan Wu, Qiuhe Peng

Department of Astronomy, Nanjing University, Nanjing 210093, China

yhzhao, zyli@nju.edu.cn

and

Zhousheng Zhang, Zili Li

Yunnan Astronomical Observatory, Kunming 650011, China

(Received ; accepted)

Abstract

We have taken a 4-day spectroscopic observation and have been conducting a 13-day photometric study of the SU UMa-type dwarf nova, ER Ursae Majoris. The mean K -amplitude for the emission lines is 54 ± 8 km s⁻¹ and γ velocity is 8 ± 4 km s⁻¹ from our spectroscopic results. A phase shift of 0.22 is also obtained.

Our photometric observation confirms superhumps in normal outbursts of ER UMa and reconciles contradictory observational results obtained by different authors. We find that superhumps possibly develop near each normal outburst maximum and fade out before the next outburst maximum. If the observed humps were not late superhumps but ordinary superhumps, much more theoretical works should be done to explain the new phenomena.

Key words: accretion, accretion disks - novae, cataclysmic variable - stars: individual (ER UMa)

1. Introduction

Cataclysmic Variables (CVs) are short-period binaries in which the Roche-Lobe-filling secondary transfers mass through the inner Lagrangian point. Most CVs are active systems with more or less change in magnitude at various time scales. SU UMa-type dwarf novae are defined as a special class of CVs with two distinctive outbursts, “normal outbursts” as in SS Cyg stars and “superoutburst” with larger amplitude and lasting 5-10 times longer. An excellent review of superoutbursts was presented by Warner (1995).

It has been extensively accepted that normal outbursts are triggered by “thermal instability” described by “S-curves” (Meyer & Meyer-Hofmeister 1981; Warner 1995), which gives the $\Sigma - T_{eff}$ relationship for each annulus in the accretion disk. And superoutbursts are ex-

plained as the result of “thermal-tidal instability” (Osaki 1989, TTI hereafter) in the disk. In this model, the tidal instability is only effective after the radii of the accretion disk grows larger than a critical value, which is satisfied exclusively in superoutburst. After the radius exceeds the critical value, the disk becomes eccentric and produces superoutbursts and “superhumps”, which are periodic variations of about 0.2-0.3 mag in light curves after superoutburst maximum.

Another interesting problem is the explanation of the negative superhumps. The most plausible model is based on the assumption of a retrograde precession of a tilted accretion disk (Patterson et al. 1993, 1997). Although the positive superhumps have been simulated numerically since the work of Whitehurst (1988), there are some difficulties to simulate the negative superhumps. In fact, all attempts to simulate negative superhumps failed in sense that they were not able to produce a significant tilt starting from a disk lying in the orbital plane (Murray & Armitage 1998; Wood et al. 2000). Once tilted, however, the accretion disk starts precession in retrograde direction (Wood et al. 2000). However, the origin of the disk tilt remains uncertain.

The studies of photometry (Kato & Kunjaya 1995; Robertson, Honeycutt, & Turner 1995) show that ER UMa is a peculiar SU UMa-type dwarf nova with short supercycles of 40-50 days in which the superoutburst lasts about 20 days. Its normal outburst has a period of 4 days. Misselt and Shafter (1995, named paper I hereafter) detected no superhump in normal outburst (see 1994 March 11 in their Figure 8). Kato and Kunjaya (1995, named paper II hereafter) also declared that no clear evidence of periodic humps with an amplitude larger than 0.05 mag was detected during a normal outburst. However, Gao et al. (1999, named paper III hereafter) found that superhumps exist in normal outbursts of ER UMa, which is not expected in TTI model. Although they claimed in paper III that “it is more likely that superhumps occasionally exist at essentially all phases of the eruption cycles of ER UMa stars”, it remains uncertain in the rising to normal maximum because of lack of observations.

Spectroscopic studies have not been performed as extensively as photometric ones. Thorstensen et al. (1997, TTBR hereafter) derived an orbital period of 0.06366 days and a semiamplitude, K , of 48 ± 4 km s⁻¹ of the radial velocity. Both spectroscopy and photometry performed simultaneously were much scarcer. We took both kinds of observations in 2004 February, and in this paper we report the spectroscopic features of the accretion disk during normal outburst and the superhumps behavior during the rise to normal outburst maximum and the development in normal outburst.

2. Observation

We took spectroscopic observations of ER UMa for 25.7 hr over 4 nights through February 27 to March 1 in 2004, using the OMR Cassegrain spectrograph attached to the 2.16 m telescope with a TEK1024 CCD camera at Xinglong Station of National Astronomical Observatory of China. A total of 63 useful spectra was obtained. The technique of observation

and data processing is similar to that in Wu et al. (2001). A 300 groove mm^{-1} grating was used, and the slit width was set to $2''$. We recorded dome flats at the beginning and end of each night. The lamp spectra were taken before and after every two star exposures and used to interpolate the coefficients of wavelength scales. A spectral resolution of 13 \AA was derived from FWHM of the lamp spectra and the rms of identified lines was 0.19 \AA using a fourth-order Legendre polynomial to fit the lines, corresponding to 12 km s^{-1} near $\text{H}\beta$.

The photometric observation of ER UMa was taken in 1999 and 2004, using a TEK1024 CCD camera attached to the Cassegrain focus of the 1.0 m reflector at Yunnan Observatory. The observation lasted for 26 hours over 6 nights through December 1999 to January 2000 and for 40 hours over 7 nights in February 2004, in each night covered well over 3-4 superhump periods of the object. Exposure times were 40, 60 or 90 s, long enough to assure good signal-to-noise ratio. A total of 1892 useful object frames were obtained through V filter. After bias subtraction and flat field correction, we removed the sky background and measured magnitudes of ER UMa and two secondary photometric standards, star 4 and star 10 in finding chart of Henden & Honeycutt (1995). We use these two standards as the comparison star (star 4) and check star (star 10), respectively, after paper III. The rms error is less than 0.02 mag. The journal of our detailed observations is summarized in Table 1.

3. Results and analysis

3.1. Average spectrum and the radial velocity

In Figure 1 we show the sum of all 63 individual spectra, which had been normalized to continuum. No radial velocity shift was applied during the combination. The spectrum presented strong Balmer emission lines and weaker He I lines from $\lambda 4471 \text{ \AA}$ to $\lambda 6678 \text{ \AA}$. There is also He II $\lambda 4686 \text{ \AA}$. Equivalent widths of spectral features are given in Table 2.

We measured the central wavelengths of $\text{H}\beta$ emission peaks with the Gaussian-fit method. Figure 2 shows the velocities folded on the orbital phase with the best-fit sinusoidal superposed. The orbital phase was calculated according to the ephemeris given by TTBR,

$$T_0 = \text{HJD}2449740.0478(8) + 0.06366(3)E \quad (1)$$

where T_0 is the time of the γ crossover from negative to positive, and E is the cycle number. The best-fit sinusoidal shows that the $\text{H}\beta$ emission has $K=54\pm 8 \text{ km s}^{-1}$, $\gamma=8\pm 4 \text{ km s}^{-1}$. TTBR obtained smaller K , $48\pm 4 \text{ km s}^{-1}$ and smaller γ , $-31\pm 3 \text{ km s}^{-1}$ from the $\text{H}\alpha$ emission lines using two-Gaussian convolution method with a separation of 1260 km s^{-1} . The large difference of γ should be mainly caused by the following reason (see next paragraph). The large phase offset of 0.22 shows that the variation of line peaks can not exactly represent the motion of the white dwarf.

The symbols in Figure 2 represent different nights. It is clear that there exist systematic discrepancies between different nights. The distribution of velocities on February 27 is almost

Table 1. Journal of observations

Date (UT)	HJD start (2,451,000+)	Duration (hr)	Exposure ^a (s)	Plates	Period (days)	Δm (mag)
Spectroscopy						
2004 Feb 27	2063.0455	1.75	1200	7
2004 Feb 28	2064.0536	7.36	1200	17
2004 Feb 29	2065.0425	8.40	900	27
2004 Mar 1	2066.0344	8.21	1200	12
Photometry						
1999 Dec 30	543.178	4.56	90	118	0.0659(20)	0.12
1999 Dec 31	544.182	4.35	60	120	0.0656(17)	0.30
2000 Jan 1	545.176	4.97	60	143	0.0643(23)	0.47
2000 Jan 2	546.177	4.51	90	75	—	~ 0.03
2000 Jan 3	547.189	4.37	90	120	0.0671(20)	0.12
2000 Jan 4	548.179	5.04	90	135	0.0663(35)	0.18
2004 Feb 23	2059.396	3.83	90	63	—	~ 0.15
2004 Feb 24	2060.344	6.50	90,60	200	—	~ 0.1
2004 Feb 25	2061.338	5.01	60,40	180	0.0686(13)	0.05
2004 Feb 26	2062.329	6.25	60	209	—	~ 0.08
2004 Feb 27	2063.369	6.25	90	171	—	0.1-0.2
2004 Feb 28	2064.333	6.12	90	197	—	0.1-0.3
2004 Feb 29	2065.335	6.01	90	161	0.0590(10)	0.4-0.15

^a Exposure time shown here is the most common one at each night.

Table 2. Equivalent Width of Spectral Lines

Equivalent		Equivalent	
Element, Rest Wavelength	Width (\AA)	Element, Rest Wavelength	Width (\AA)
He ϵ λ 3970	16.6	He I λ 3889	8.2
H δ λ 4101	18.6	He I λ 4471	5.1
H γ λ 4340	24.9	He I λ 4922	3.7
H β λ 4861	27.1	He I λ 5015	3.8
H α λ 6563	33.7	He I λ 5876	7.6
He II λ 4686	3.9	He I λ 6678	4.4

below the sinusoidal. Those on February 28 and 29 moved upper and upper with time, and then down again on March 1. The mean values of velocities on different nights are -64 km s^{-1} , 4 km s^{-1} , 38 km s^{-1} and -10 km s^{-1} , following the date sequence. This result is very reasonable if we accept that the outer part of the accretion disk is eccentric and precessing. A detailed analysis of variation of mean velocity produced by an eccentric precessing outer disk at different phase was given by Wu et al. (2001) and Zhao et al. (2005, 2006). Since our data were all taken in a normal outburst (see §3.2.2), it is naturally believed that the outer disk of ER UMa was eccentric and precessing during its *normal* outburst. Hence, it is not surprised that the γ velocity of TTBR, which is measured in quiescence, is much smaller than that of ours.

3.2. Superhumps in the decline part of outbursts

3.2.1. The outbursts occurred in 1999-2000

Figure 3a shows the photometric data recorded in December 1999 and January 2000. The light curve covers the decline part of an outburst and another almost complete outburst. The amplitude of the second outburst is about 2.2 mag and it lasts about 4 days. But we could not make sure whether these two outbursts are normal outburst or superoutburst. For the first outburst, it is incompletely observed and it may be a superoutburst or a normal outburst. For the second outburst, the mean decline rates are $0.73 \text{ mag day}^{-1}$ and $0.95 \text{ mag day}^{-1}$, for January 3 and 4, respectively. These values are similar to those of normal outbursts presented in Paper III and in this paper (see the following section). Therefore, we treat it as normal outburst based on its duration and fading rate.

There are apparent oscillations in all days except in January 2. Figure 4 shows the period-theta diagrams derived from PDM method (Stellingwerf 1978) for two segments of data, (a) covering December 30, 31 and January 1 (data A hereafter), (b) covering January 3 and January 4 (data B hereafter). They give periods, P_A ($0.06562(14) \text{ d}$) and P_B ($0.06638(35) \text{ d}$), $(3.1 \pm 0.2)\%$ and $(4.3 \pm 0.5)\%$ larger than the orbital period of 0.06366 d (Thorstensen and Taylor 1997), respectively. The mean errors of the periods are the most pessimistic estimations derived from the method of Fernie (1989). Fitting sinusoidals to the two segments of data gives two ephemerises,

$$T_0(max) = HJD2451543.14666 + 0.06562n \quad (2)$$

$$T_0(max) = HJD2451547.15245 + 0.06638n \quad (3)$$

where T_0 is the time at phase zero of fit sinusoidals, n is the cycle number. We also computed period-theta diagram for individual data series. The results of period determination and full amplitudes of magnitude variation (Δm , derived from fitting sinusoidal to data in Figure 3a) are also listed in Table 1. Although the errors for data of each day are rather large, there is a trend that period decreases with time increasing within each outburst.

We tried to find whether there is a unique stable period throughout the whole light curve, i.e., whether the difference between the periods of data A and data B derived above

is due to intrinsic change or period determination error. The period-theta diagram for the whole curve is shown in Figure 4c. At the first glance, there is really a period ($P_C=0.06572$ d) which fits the whole light curve. However, we found that it was not the case. We tried to add $(n\pm r)P_C$ (n is an integer, r is a real number from 0 to 0.5) to time abscissa of data B. There was a single dominant peak near P_C in derived period-theta diagram when r is approximately less than 0.2. And there are two peaks at P_A and P_B when r is greater than 0.2. It means that when two segments data are of different period as in our case, there is a probability of 40% to obtain a single peak. Because the errors of P_A and P_B are the most pessimistic estimations and the difference of them is larger than the errors, we believe there is no unique period which fits the whole light curve. In fact, unstable period is a well-known property of superhump (Warner 1995). The amplitudes of the oscillations range from 0.12 mag in December 30 to 0.48 mag in January 1. Considering the periods and amplitudes of the modulations, we identify them as superhumps.

Figure 5 shows magnitude variation versus superhump phase calculated according to equation (2) and equation (3), respectively. The light curve of January 4 is double-peaked. This feature suggests that the structure of the accretion disk is more complex than a simple eccentric disk in the day.

3.2.2. *The normal outburst occurred in 2004*

Figure 3b is the light curve obtained during 2004 February 23-29. The full amplitude of this outburst is about 2.5 mag. The average rising and decline rate are 2.5 and 0.7 mag day⁻¹, respectively. It is easily obtained that the period of this normal outburst is about 6 days, which is 2 days longer than the usual 4 days (Paper I; Paper II; Paper III). From the light curve of AAVSO¹, we can find that the mid time of our observation was just about 10 days before the occurrence time of a superoutburst.

Figure 6 shows the daily light curves with linear trend removed. The periodogram and window spectrum (Scargle, 1982) of data covering February 25-28 are shown in Figures 7a₁ and 7a₂, respectively. There are two peaks at frequencies 13.938 circles day⁻¹ and 14.956 circles day⁻¹. But from the periodgram of data obtained in February 25, as shown in Figure 7b₁, we can see there is only one high peak at a frequency 14.566 cycles d⁻¹. So we believe that the frequency of 14.956 cycles d⁻¹ is the true superhump frequency and the frequency of 13.938 cycles d⁻¹ is an alias and the corresponding period of 0.06686(09) d is $(5.0\pm0.15)\%$ larger than the orbital period.

As shown in Figure 6, the modulations in February 25, when the observational run was just after the outburst maximum, are the smallest. The middle panel in Figure 8 (a enlarged view of Figure 6) shows more clearly that the magnitude variation is about 0.05 mag. Moreover, the superhump amplitude is increasing till near the end of the outburst (see Table 1).

¹ <http://www.aavso.org>

The light curve shown in the lower panel in Figure 8 shows that the superhumps in February 29 are diminishing. At the beginning of the run, there appears to be a modulation with full amplitude about 0.4 mag. Then it becomes 0.3 mag and till about 0.15 mag at the end of the run. The periodgram and window spectrum are shown in Figures 9a and 9b, respectively. The high peak is at a frequency $16.937 \text{ circles day}^{-1}$. It seems to be a negative superhump with a period of 0.05904(55) day, $(7.3 \pm 0.9)\%$ smaller than the orbital period. Paper III found negative superhump during early rising of a superoutburst with a period 0.0589 days, which is very consistent with our result.

3.3. *Fading superhump in the rising to normal maximum*

Figure 5 shows that magnitude variation in January 2 is the smallest. A magnified view of the variation is shown in Figure 10. Within the first superhump period, there is a modulation of about 0.06 mag. Within the second superhump period, there is very small variation approximate to measuring error if ignoring linear trend. Even considering this trend, the amplitude is much smaller than that in the first superhump period. Therefore, it is possible that the superhump begins to appear near the outburst maximum and disappear before next outburst maximum.

Figure 3b shows the light curve in February 24 is the original data. At the first glance the modulations only exist at the beginning of the run. In fact, after cubic polynomial trend subtraction, as shown in the upper panel in Fig 8 (the magnified view of Figure 6), the modulations of about 0.1 mag exist along the whole run. We can see roughly in Figure 8 that the period of modulation at the second half of this run became about two times greater than the one at the first half. Period analysis indicates crudely that these two periods are 0.07516(155) d and 0.11857(334) d, respectively.

According to the magnitudes and rising rates in paper I and II, Figure 3b shows rough positions of their observations in a normal outburst (the symbol “star” represents estimated position of maximum light). The observation of paper I mentioned above is taken in the middle of the rise to the maximum of a normal outburst, which is very similar to our observation on February 24. And it can be seen that a modulation (~ 0.1 mag) presents in the light curve (see 1994 March 11 in their Figure 8). This is consistent with our light curve shown in Figure 3b. Moreover, a close inspection of Figure 5 in paper II suggests that the observing run is also in the rise and right before the maximum of the normal outburst. A wave (~ 0.05 mag) with a period near superhump period is gradually disappearing. From Figure 5 of paper III, we can see that the rise to the normal maximum occurred in daytime and they missed it. So the observations of the three groups are all coincident with the observational results in this paper. Combining the facts described above and this paper, it seems to be that superhump begins to appear near normal maximum and disappears before the next normal maximum.

Therefore, superhump behavior described in this paper clarifies the problem (see §1).

First, it confirms that there are actually superhumps in normal outbursts of ER UMa. Second, superhump in the decline part might set out near (maybe at or a little later than) the normal maximum. Third, superhumps possibly disappear before the next normal maximum.

4. Discussion

In SU UMa-type dwarf novae, two types of humps, which have periods slightly longer than the orbital periods, have been observed. These humps are (ordinary) superhumps (Warner 1995) and late superhumps (e.g., vogt 1983; Hessman et al. 1992). In this section, we discuss the nature of our observed humps during normal outbursts in ER UMa.

4.1. *The late superhumps*

In the manner of Vogt’s (1982) early model for ordinary superhumps, Osaki (1985) and Whitehurst (1988) put forward that the eccentric disk survives for several days after the end of a superoutburst. Thus, the modulation of the hotspot brightness, which is caused by the stream impacts the disc at varying depth in the white dwarf potential, produces late superhumps. But Hessman et al. (1992) pointed out that the eccentricity determined in OY Car is too small to produce sufficient modulation. They suggested that there should be considerable variation in surface density and scale height around the rim of an eccentric disc, and this should cause variation in the appearance of the hotspot. However, Rolfe et al. (2001) find out that brightness of the hotspot varies with $|\Delta\mathbf{V}|^2$, which supported the former model.

According to the hotspot model, the modulations would diminish in the rising phase of an outburst and develop in the fading phase. This is due to that the emission from the accretion disk becomes more dominant after the onset of outburst. Thus, the contribution from the hotspot is getting weaker and weaker. In the fading phase, a reversed effects happen. In this respect, our observational phenomena could be taken for late superhumps. However, we cannot make a conclusion that they are late superhumps since (1) there is no superoutburst observed; (2) the 0.5 phase shift, which is the basic definition of late superhump, cannot be investigated.

4.2. *The ordinary superhumps*

The TTI model was proposed to explain bimodal outbursts of SU UMa stars (Osaki 1989). Many numerical simulations (Hirose & Osaki 1990; Whitehurst 1994; Kunze et al. 1997; Murray 1998; Truss et al. 2001) showed that thermal-tidal instability model was very successful on explaining behaviors of SU UMa stars. Based on the model and adopting a mass transfer rate 10 times higher than that expected in the standard theory of the evolution of cataclysmic variables, Osaki (1995) reproduced the light curve of ER UMa. However, it should be noted that these simulations only can demonstrate that the model is able to reproduce the phenomena known in the past, in which the most important is existence of superhumps only

after supermaximum of SU UMa stars.

Paper III found superhumps in normal outburst and suggested that superhumps existed essentially in all phase of a supercycle. Hellier (2001) suggested that eccentricity might last after the end of superoutburst in low mass ratio systems and the long-life eccentricity caused superhumps observed after the end of superoutbursts. Based on the observations in paper III, Buat-Ménard and Hameury (2002) supported this kind of “decoupling” and proposed normal superhumps in ER UMa stars should be “permanent” caused by permanent eccentricity.

We find that superhump is both in the rise and decline part of a normal outburst. Our observation also demonstrates that superhumps disappear in a part of the rise to normal maximum. If the observed humps were ordinary superhumps, these suggest that superhump (eccentricity) undergoes development and disappearance in a cycle of normal outburst. In this case, long-life eccentricity can’t explain superhumps in normal outbursts of ER UMa. Superhump is not permanent in ER UMa, either. Because superhumps develop in each normal outburst, we have to investigate the relation between eccentricity (superhump) and superoutburst further.

More observations of other ER UMa-type stars should be taken to examine whether superhumps in normal outbursts are common in this kind of system and to examine whether the superhumps really disappear in a part of the rise to outburst maximum. Second, further investigations on the relation between superhump and superoutburst are needed.

Acknowledgments: The authors are grateful to the anonymous referee for his/her carefully reading of the manuscript and thoughtful comments. We would like to thank the Optical Astronomy Laboratory, Chinese Academy of Sciences and Dr. Peisheng Chen of Yunnan Astronomical Observatory for scheduling the observations. This work is supported by grants 10173005 and 10221001 from the National Natural Science Foundation of the People’s Republic of China.

References

- Buat-Ménard, V., & Hameury, J.-M. 2002, A&A, 386, 891
Gao, W., Li, Z., Wu, X., Zhang, Z., & Li, Y. 1999, ApJ, L55
Ferne, J. D. 1989, PASP, 101, 225
Hellier, C. 2001, PASP, 113, 469
Henden, A. A., & Honeycutt, B. K. 1995, PASP, 107, 324
Hirose, M., & Osaki, Y. 1990, PASJ, 42, 135
Kato, T., & Kunjaya, C. 1995, PASJ, 47, 163
Kunze, S., Speith, R., & Riffert H. 1997, MNRAS, 289, 889
Meyer, F., & Meyer-Hofmeister, E. 1981, AAp, 104, L10
Misselt, K. A., & Shafter, A. W. 1995, AJ, 109, 1757
Murray, J. R. 1998, MNRAS, 297, 323
Murray, J. R., & Armitage, P. J. 1998, MNRAS, 300, 561

- Osaki, Y. 1985, A&A, 144, 369
- Osaki, Y. 1989, PASJ, 41, 1005
- Osaki, Y. 1995, PASJ, 47, L11
- Patterson, J., Kemp, J., Saad, J., Skillman, D. R., Harvey, D., Fried, R., Thorstensen, J. R., & Ashley, R. 1997, PASP, 109, 468
- Patterson, J., Thomas, G., Skillman, D. R., & Diaz, M. 1993, ApJS, 86, 235
- Robertson, J. W., Honeycutt, R. K., & Turner, G. W., PASP, 107, 443
- Rolfe, D. J., Haswell, C. A., & Patterson, J., MNRAS, 324, 529
- Scargle, J. D. 1982, ApJ, 263, 835
- Stellingwerf, R. F. 1978, ApJ, 224, 953
- Thorstensen, J. R. & Taylor, C. J., 1997, PASP, 109, 477
- Truss, M. R., Murray, J. R., & Wynn, G. A. 2001, MNRAS, 324, L1
- Vogt, N., 1982, ApJ, 252, 653
- Vogt, N., 1983, A&A, 118, 95
- Warner, B. 1995, Cataclysmic Variable Stars (Cambridge: Cambridge Univ. Press)
- Whitehurst, R. 1988, MNRAS, 232, 35
- Whitehurst, R. 1994, MNRAS, 266, 35
- Wood, M. A., Montgomery, M. M., & Simpson, J. C. 2000, ApJ, 535, L39
- Wu, X., Li, Z., & Gao, W. 2001, ApJ, L81
- Zhao, Y. H., Li, Z. Y., Wu, X. A., & Peng, Q. H., ChJAA, 2005, 5, 601
- Zhao, Y. H., Li, Z. Y., Peng, Q. H., Wu, X. A., Shang, Z. S., & Li, Z. L., AJ, 2006, in press (astro-ph/0511468)

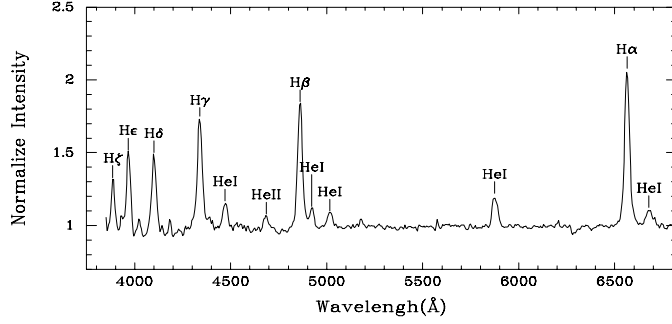


Fig. 1. The sum of all 63 spectra, showing strong Balmer emission lines. The helium emission lines from $\lambda 4471$ to $\lambda 6678$ can be also seen clearly.

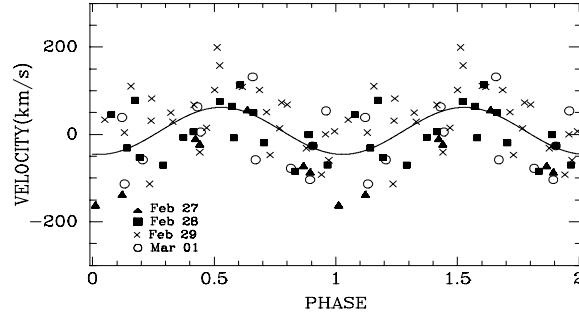


Fig. 2. Radial velocity of the emission line $H\beta$ and best fit sinusoidal. Phase computed according to the ephemeris expressed by eq. [1]. The velocities measured in different days presented in the figure with different symbols, from which we would like to see the variation of the velocities when the disk at its different precessing phase.

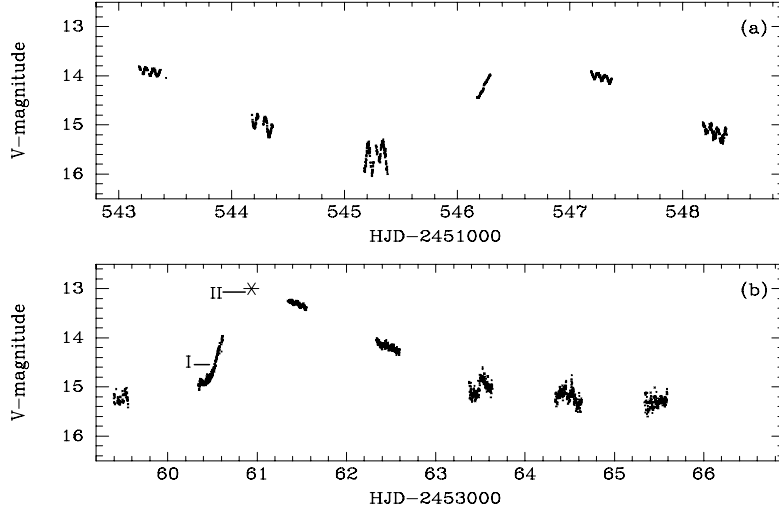


Fig. 3. All of our photometric data. (a) Data recorded in 1999 December and 2000 January. It shows the decline part of a normal outburst and another almost complete normal outburst. Modulation of 0.1-0.5 mag clearly present in the light curve except in January 2. (b) Data recorded in 2004 February. It shows a complete normal outburst. We can see clearly that the period of this normal outburst is 6 days, which is 2 days longer than usual period of ER UMa. The total amplitude of this outburst is about 2.5 mag. The symbol “star” represents estimated position of maximum light. The horizontal lines, ‘I’ and ‘II’ roughly represent phase of observations of paper I and paper II in a normal outburst, respectively.

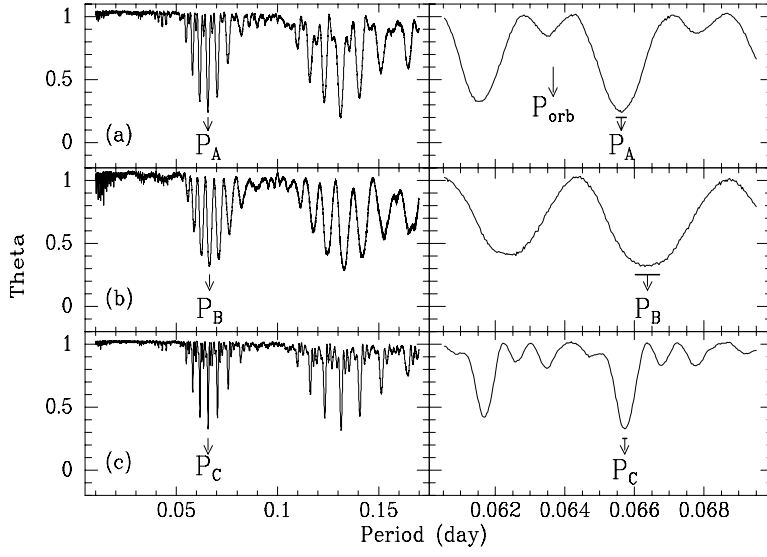


Fig. 4. Period-theta diagrams of three series of data: (a) From December 30 to January 1, (b) From January 3 to January 4, (c) the whole light curve excluding January 2. In the right is magnified view of each diagram. The horizontal lines at the ends of the arrows represent the most pessimistic error bars, so we identify the modulations in the light curve as superhumps. Although there is a single peak in (c), we believe that there is no unique period can span the whole light curve (see the text).

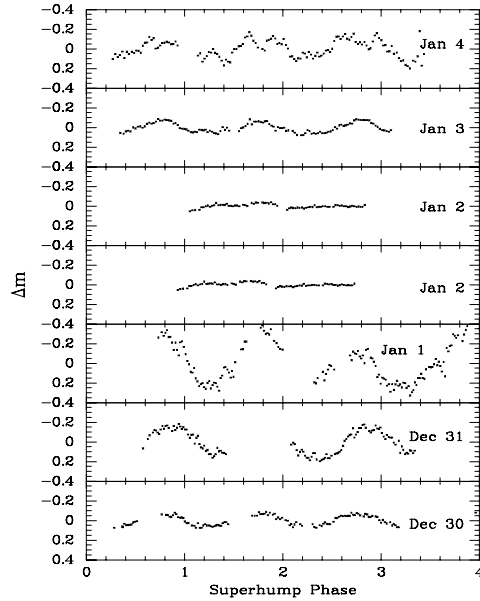


Fig. 5. Magnitude variation versus superhump phase. Linear trend has been removed. Superhump phase in the lower 4 panels are computed according to equation (2), that in the higher 3 panels are computed according to equation (3). Modulation in January 2, if any, is the smallest.

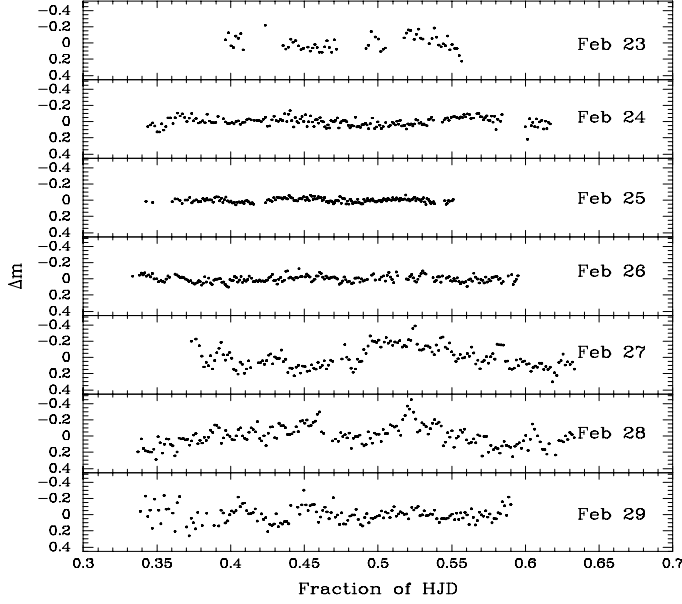


Fig. 6. Daily light curves recorded in 2004 February. Linear trend has been removed from all data series except that a cubic polynomial trend has been subtracted in Feb 24. Modulations of ~ 0.1 mag and 0.05 mag clearly present in February 24 and 25, the time rising to and after normal maximum, respectively. And the amplitude increases during the decline part of the outburst. In February 29, a wave (~ 0.2 mag) is gradually disappearing.

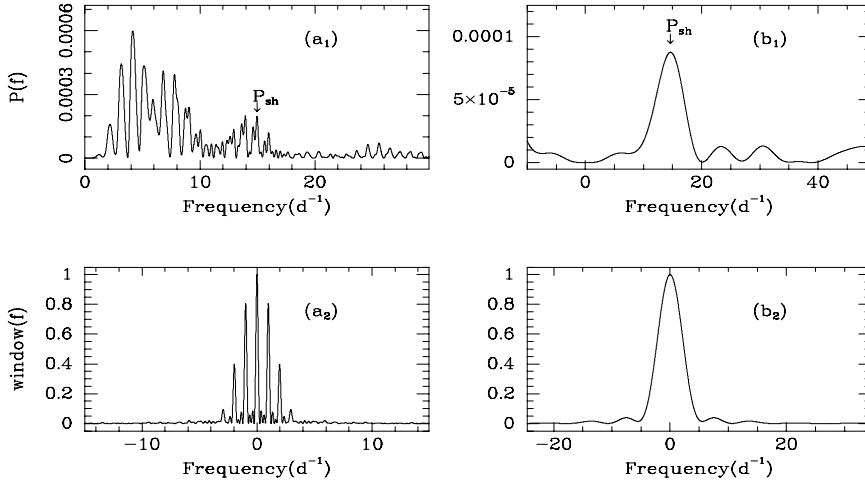


Fig. 7. Periodogram of data series from February 25 to 28. (a_1) The power spectrum of data series covered February 25,26,27,28 (data C). (a_2) The window spectrum of data C. (b_1) The power spectrum of photometric data recorded in February 25 (data D). (b_2) The window spectrum of data D.

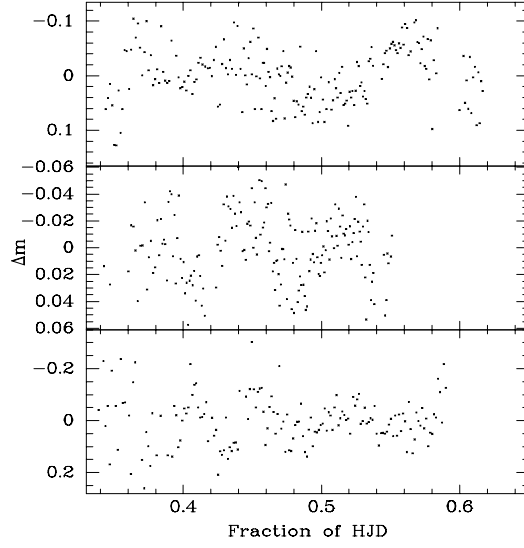


Fig. 8. A magnified view of magnitude variation in February 24 (upper panel), February 25 (middle panel) and February 29 (lower panel) shown in Figure 6. Although modulations present in all three light curves, the amplitudes are obviously varying. In February 24, the full amplitude is about 0.1 mag, but it becomes 0.05 mag in February 25, just before and after the outburst maximum respectively. In February 29, when the outburst is close to the end, modulations are weakening quickly. The full amplitude is from 0.4 mag to 0.15 mag.

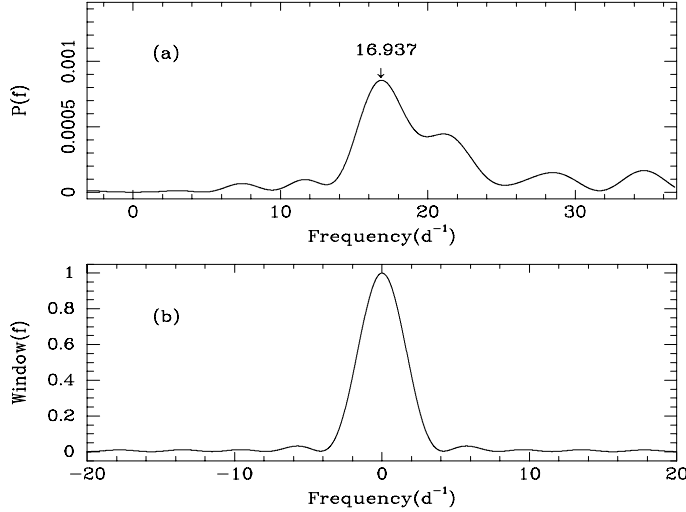


Fig. 9. Periodgram of photometric data obtained in February 29. (a) The power spectrum. (b) The window spectrum.

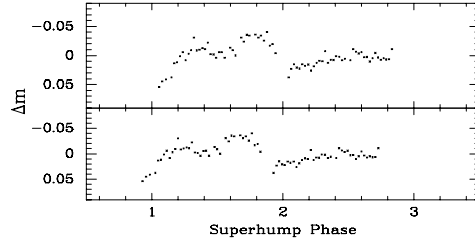


Fig. 10. A magnified view of magnitude variation in January 2 shown in Figure 5. There is a modulation (~ 0.06 mag) in the first superhump period and no modulation is detected in the second period.